Nanoscopic Vibrations of Bacteria with Different Cell-Wall Properties Adhering to Surfaces under Flow and Static Conditions

Lei Song, Jelmer Sjollema, Prashant K. Sharma, Hans J. Kaper, Henny C. van der Mei, and Henk J. Busscher*

Department of Biomedical Engineering, University of Groningen and University Medical Center Groningen, Antonius Deusinglaan 1, 9713 AV Groningen, The Netherlands

ABSTRACT Bacteria adhering to surfaces demonstrate random, nanoscopic vibrations around their equilibrium positions. This paper compares vibrational amplitudes of bacteria adhering to glass. Spring constants of the bond are derived from vibrational amplitudes and related to the electrophoretic softness of the cell surfaces and dissipation shifts measured upon bacterial adhesion in a quartz-crystal-microbalance (QCM-D). Experiments were conducted with six bacterial strains with pairwise differences in cell surface characteristics. Vibrational amplitudes were highest in low ionic strength suspensions. Under fluid flow, vibrational amplitudes were lower in the direction of flow than perpendicular to it because stretching of cell surface polymers in the direction of flow causes stiffening of the polyelectrolyte network surrounding a bacterium. Under static conditions (0.57 mM), vibrational amplitudes of fibrillated *Streptococcus salivarius* HB7 (145 nm) were higher than that of a bald mutant HB-C12 (76 nm). Amplitudes of moderately extracellular polymeric substance (EPS) producing *Staphylococcus epidermidis* ATCC35983 (47 nm) were more than twice the amplitudes of strongly EPS producing *S. epidermidis* ATCC35984 (21 nm). No differences were found between *Staphylococcus aureus* strains differing in membrane cross-linking. High vibrational amplitudes corresponded with low dissipation shifts in QCM-D. In streptococci, the polyelectrolyte network surrounding a bacterium is formed by fibrillar surface appendages and spring constants derived from vibrational amplitudes decreased with increasing fibrillar density. In staphylococci, EPS constitutes the main network component, and larger amounts of EPS yielded higher spring constants. Spring constants increased with increasing ionic strength and strains with smaller electrophoretically derived bacterial cell surface softnesses possessed the highest spring constants.

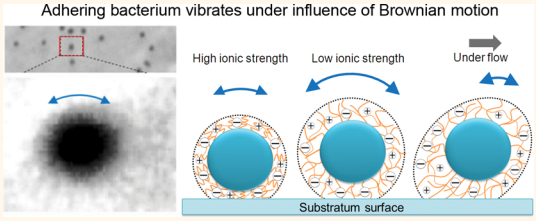

KEYWORDS: biofilm · bacterial vibration · spring constants · Brownian motion · polyelectrolyte network stiffening · cell surface softness · bacterial adhesion

Biofilm formation is ubiquitous since bacteria have the ability to adhere to virtually all synthetic and natural surfaces in either environmental, industrial, or biomedical settings.[1−3] Biofilms allow essential chemical-transfer processes to occur between resident bacteria and their external world, while providing protection to their inhabitants.[4,5] Adhesion is the most crucial step in biofilm formation, and it is realized more and more that the characteristics of the adhesive bond impact bacterial behavior in terms of morphological, genomic, and proteomic responses.[6,7] Moreover, bacteria adhering directly to a substratum surface constitute a layer that links all other bacteria growing on top of it to the substratum. As a consequence, many different experimental systems have been developed to measure the ability of bacteria to adhere to substratum surfaces.[8−12]

Flow displacement systems can probably be considered as the most quantitative ones allowing precise control of the flow and therewith of the mass transport preceding bacterial adhesion.[12] Moreover, in combination with real-time imaging, the kinetics of bacterial adhesion can be determined.[13] Although many papers[14−16] are based on employing flow displacement systems with real-time image analysis options, there is a special trait demonstrated by bacteria adhering to a substratum surface that has only been reported on in two similar studies on

* Address correspondence to h.j.busscher@umcg.nl.

Received for review June 3, 2014 and accepted July 15, 2014.

Published online July 15, 2014
10.1021/nn5030253

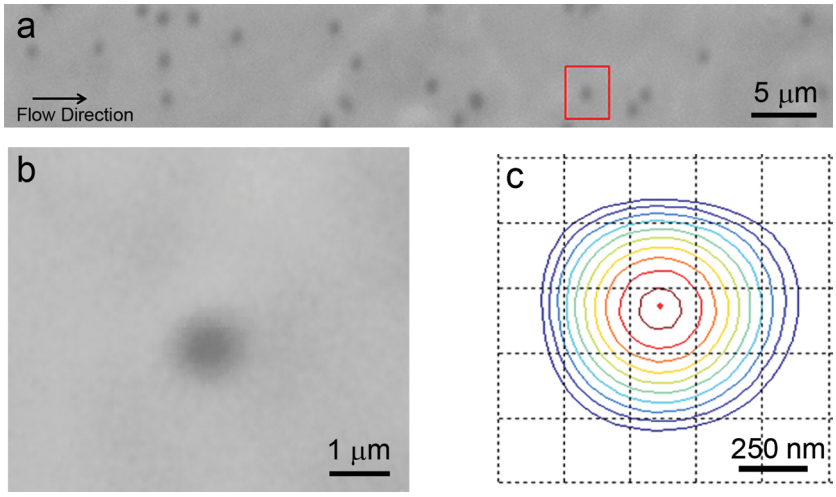

Figure 1. Outline of the method applied to determine bacterial positions. (a) Snap-shot image of *S. salivarius* HB7 adhering on the glass substratum under fluid flow at an ionic strength of 0.57 mM obtained by phase contrast microscopy. (b) Enlarged image of the bacterium in the red box (see (a)). (c) Concentric elliptic contour lines calculated from (b). The red point in the center of the concentric ellipses represents the position of an adhering bacterium and is used to calculate the vibrational amplitude, either in the direction of fluid flow or perpendicular to it or averaged over all directions when measured under static conditions.

adhesion of inert, nonbiological particles and red blood cells:[17,18] adhering bacteria show nanoscopic, random vibrations around their equilibrium positions (Figure 1 and see the video in the Supporting Information). Superficially, these vibrations of adhering bacteria bear similarity to the nanoscopic motions of living bacteria that can be sensed by the cantilever of an atomic force microscope (AFM),[19] but in our experience both dead and living bacteria exhibit nanoscopic vibrations when adhering, ruling out a metabolic cause. This is supported by the observation that inert, nonbiological particles[17,18] adhering to surfaces also exhibit nanoscopic vibrations. The lack of attention for this phenomenon in bacterial adhesion is amazing, as analysis of the vibrations exhibited by adhering particles enables calculation of the spring constant of the bond between particles and substratum surfaces.[17,18] More detailed information on the spring constants of the bond between bacteria and substratum surfaces is direly needed, as the viscoelasticity of the bond plays an important role in determining the ease with which adhering bacteria can be removed from substratum surfaces[20,21] or protect themselves against mechanical challenges in general.

The outermost bacterial cell layer in contact with substratum surfaces is composed of a variety of different surface appendages and a matrix of extracellular polymeric substances (EPS) containing, among others, polysaccharides, lipids, and proteins, tied together by extracellular DNA.[22] The outermost bacterial cell layer has been demonstrated to behave as a polyelectrolyte layer with a strain-specific "softness" that can be measured through particulate microelectrophoresis of bacteria suspended at different ionic strengths.[23] This relatively soft, outermost layer envelopes a more rigid, hard core made of cross-linked peptidoglycan. The peptidoglycan layer is relatively thick in Gram-positive bacteria as compared to Gram-negative ones.

The aim of this paper is to investigate the conditions (ionic strength and absence or presence of fluid flow) under which nanoscopic vibrations of adhering bacteria occur and to analyze the vibrational amplitudes to yield spring constants of their adhesive bond with a substratum surface together with the frequencies of bacterial vibration. Such information has never been obtained before, and it is unknown to which properties of the bacterial cell surface these spring constants and frequencies would relate, if to any at all. In line with the polyelectrolyte nature of the outermost bacterial layer,[23,24] we search to relate the spring constants of the bonds with the electrophoretic softness of the layer. The electrophoretic softness of a bacterial cell surface can be derived from measurements of the bacterium's electrophoretic mobility at different ionic strengths and pertains to the permeability of the outermost 5−10 nm of the cell surface to fluid flow.[23] In addition, viscoelasticity of the adhesive bond between bacteria and a substratum surface is analyzed at different ionic strengths using a quartz crystal microbalance with dissipation (QCM-D).[25,26] In QCM-D, bacteria adhering to an oscillating crystal are brought into resonance and dissipate energy depending on the bond characteristics.[27]

Although over the past decades we have observed (but never published on) vibrations of adhering bacteria in a large variety of rod-shaped, coccal, and both Gram-positive and Gram-negative strains under different environmental conditions, the current study is confined to three entirely different pairs of coccal, Gram-positive strains, with pairwise interesting differences in cell-wall features: (1) *S. salivarius* HB7 and HB-C12 representing two isogenic mutant strains that differ in their possession of fibrillar surface appendages;[28]

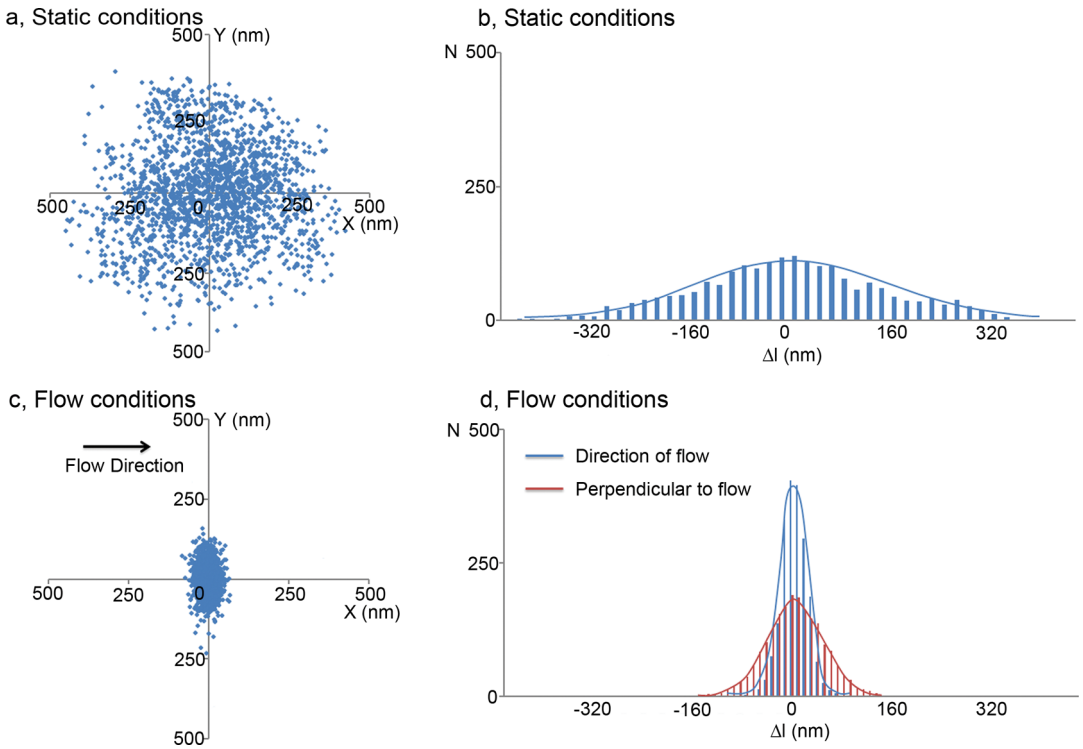

Figure 2. Examples of position maps (panels a and c) of a single, adhering bacterium (*S. salivarius* HB7 at 0.57 mM) at various time points under static conditions and under fluid flow, together with corresponding distribution histograms of bacterial displacement from its equilibrium position, Δl (panels b and d). Distribution histograms were fitted to a Gaussian function.

(2) *S. epidermidis* ATCC35983 and ATCC35984, known as moderate and strong producers of extracellular polymeric substances, respectively;[29] and (3) *S. aureus* NCTC8325-4 and its isogenic mutant NCTC8325-4 Δ*pbp-4* differing in their degree of peptidoglycan cross-linking.[30]

This choice of strains enables us to determine the influences of outermost layers of fibrillar structures and EPS, as well as of a possible influence of the rigidity of the peptidoglycan layer on vibrations of adhering bacteria. Also, coccal bacteria allow easier determination of vibrational amplitudes than rod-shaped ones.

RESULTS

Analyses of the Vibrational Amplitudes of Adhering Bacteria. Figure 2 shows examples of bacterial position maps (Figure 2a,c) and corresponding distribution histograms (Figure 2b,d) of the displacement of a single, adhering bacterium at different points in time from its equilibrium position under static conditions and under fluid flow during adhesion to glass. For both static and flow conditions the distribution of bacterial positions followed a nearly perfect fit to a Gaussian distribution function and by taking their half width at half-maximum as the vibrational amplitude of an adhering bacterium, we determined the vibrational amplitudes of the different strains involved in this study. Vibrational amplitudes were higher under static conditions than under fluid flow for all strains, but this was only statistically significant ($p < 0.05$, Student t test) at low ionic strengths (Figure 3). Under fluid flow, amplitudes were generally more perpendicular to the flow than in the direction of flow, a difference that was highest at low ionic strength. Despite the inclusion of 30 randomly selected individual bacteria in each experiment, standard deviations were relatively high and could not be significantly decreased by increasing the number of bacteria included. This suggests that there is considerable diversity in the way individual bacteria of a given strain attach to a surface. Nevertheless, the differences between the vibrational amplitudes of strains making up a pair were statistically significant and most strongly expressed at low ionic strength. The fibrillated streptococcal strain, *S. salivarius* HB7, had higher vibrational amplitudes than its bald mutant strain *S. salivarius* HB-C12 under both static conditions and fluid flow. Moderately EPS-producing *S. epidermidis* ATCC35983 demonstrated significantly ($p < 0.05$, Student t test) higher vibrational amplitudes than *S. epidermidis* ATCC35984, a strongly EPS producing strain. Under fluid flow, vibrational amplitudes of *S. aureus* NCTC8325-4 and its isogenic mutant *S. aureus* NCTC8325-4 Δ*pbp-4*, deficient in peptidoglycan cross-linking were not significantly different, but under static conditions the vibrational amplitude of the mutant strain was significantly ($p < 0.05$, Student t test) higher than that of its wild-type, parent strain.

Spring Constants of the Bond between Adhering Bacteria and a Substratum Surface Derived from Analyses of Vibrational Amplitudes. The spring constants of the bonds between

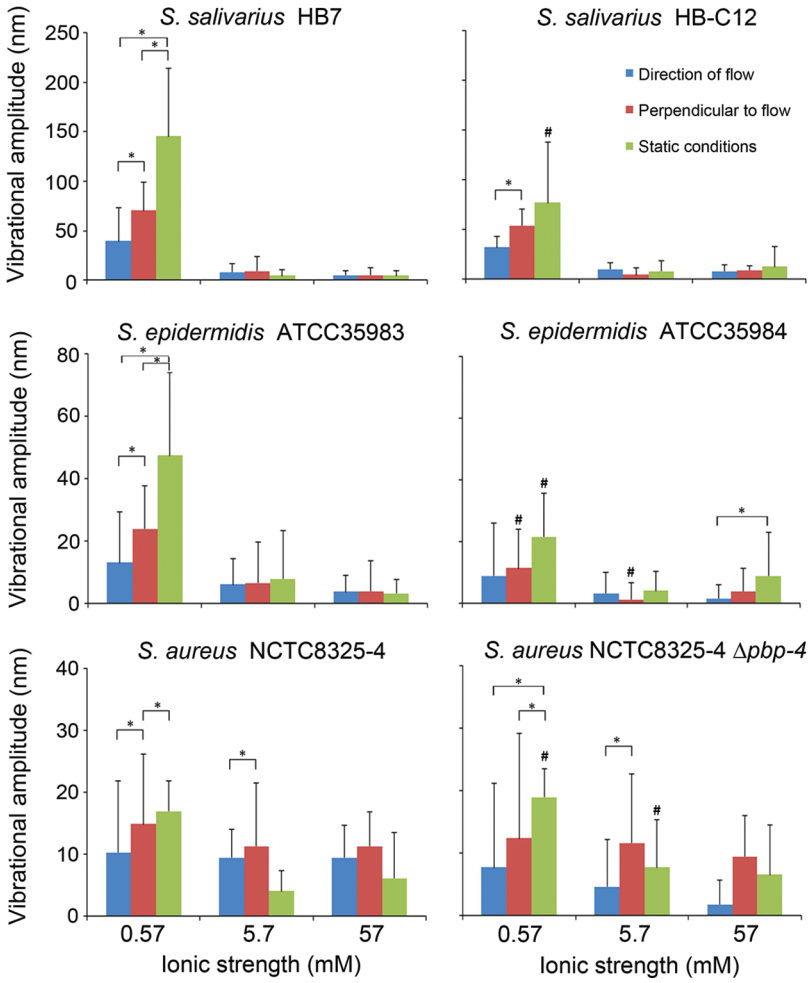

Figure 3. Vibrational amplitudes of bacteria adhering to glass surfaces at different ionic strengths for three pairs of strains under static conditions and under fluid flow. Error bars indicate standard deviations over three experiments with separately cultured bacteria. For each experiment, 30 randomly selected adhering bacteria were analyzed. ∗ indicate significant differences between vibrational amplitudes under static conditions and under fluid flow, while # indicate significant differences between vibrational amplitudes of the strains making up a pair.

the different bacterial strains and a glass substratum were derived according to eq 4 (see the Materials and Methods) from the Gaussian distributions fitted to the bacterial displacement histograms and are summarized in Figure 4. Higher vibrational amplitudes were accompanied by smaller spring constants (compare Figures 3 and 4). Accordingly, spring constants derived from vibration analysis at low ionic strength (0.57 mM) were smaller than occurring at higher ionic strengths (57 mM) and depending on whether derived under static conditions or under fluid flow. Under fluid flow, vibrational amplitudes were smaller than under static conditions, regardless of the direction of flow. The influence of fluid flow on the values of the spring constants derived suggests that stiffening of the polymer network surrounding a bacterium takes place when the bond is sufficiently stretched.[31]

Frequencies of Vibration of Adhering Bacteria and Autocorrelation Functions. In order to determine whether the frequency of video-capturing (60 Hz) is adequate for monitoring the bacterial vibrations and calculating their amplitudes, autocorrelation functions were determined of several time series of bacterial displacements (see Figure 5a,b for examples). For the example shown in Figure 5b, a significant autocorrelation over a period of time in the order of 0−1 s (i.e., 0−1 Hz) was found, showing that the frequency of video-capturing is adequate for monitoring the bacterial vibrations and for calculating their amplitudes. Next, a Fourier transform analysis was carried out on the time series of bacterial displacements in order to determine the frequency spectrum of bacterial vibrations. Large differences existed in the frequency spectra of different individual, adhering bacteria of the same strain (see Figure 5c−l). Nevertheless, high amplitudes of Fourier components were found for frequencies up to 5 Hz both for different representatives of one strain (Figure 5c−l), as well as for different strains involved in this study (Figure 6).

Bacterial Cell Surface Softness and QCM-D Bond Characteristics. Figure 7 compares the cell surface softness of the different bacterial strains and the dissipation characteristics of their bond with the substratum in a pairwise

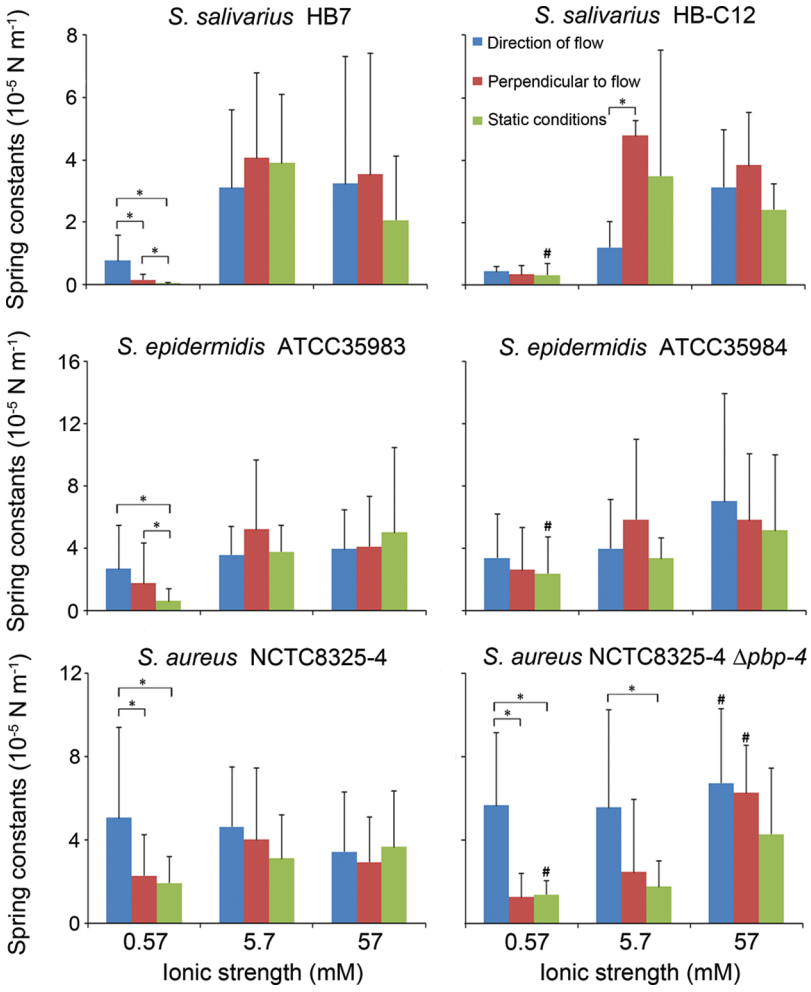

Figure 4. Spring constants of bacteria adhering to glass surfaces at different ionic strengths for three pairs of strains under static conditions and under fluid flow. Error bars indicate standard deviations over three experiments with separately cultured bacteria. For each experiment, 30 randomly selected adhering bacteria were analyzed. ∗ indicate significant differences between vibrational amplitudes under static conditions and under flow, while # indicate significant differences between vibrational amplitudes of the strains making up a pair.

manner. The fibrillated streptococcal strain displayed a significantly higher cell surface softness ($p < 0.05$, Student t test) than its bald mutant, while also the moderately EPS producing *S. epidermidis* strain had a softer cell surface than its strong EPS producing counterpart ($p < 0.05$, Student t test). No significant differences in cell surface softness were found for the pair of isogenic *S. aureus* strains (Figure 7a). The dissipation shifts, ΔD, at the first overtone for bacteria adhering to the QCM-crystal surfaces, all displayed a significant increase ($p < 0.05$, Student t test) with increasing ionic strength, indicating that higher ionic strengths were associated with higher vibrational damping (smaller amplitudes). However, there were no significant differences in dissipation shifts between the strains making up a pair (Figure 7b), except for the fibrillated pair.

DISCUSSION

Determination of the viscoelastic properties of the bond between adhering bacteria and a substratum surface constitutes a challenge of great practical and fundamental importance. AFM evaluation of the bacterial response to an applied force or imposed deformation exerted by nanoscopic AFM tips have indicated that such bonds are viscoelastic in nature.[32,33] Bacteria have also been wrenched between an AFM cantilever and a substratum surface and the dependence of the resulting deformation on the loading force has been used to derive reduced Young's moduli.[34] Reduced Young's moduli of an assumed cylindrical contact volume between an adhering bacterium and a substratum surface ranged between 8−47 kPa. Bacterial cell surfaces possessing less fibrillar surface appendages, producing less EPS or with a higher degree of cross-linked peptidoglycan layer, were more rigid. Peptidoglycan cross-linking in isogenic mutants, however, should have no direct effect on the outermost cell surface layer and its interaction with substratum surfaces (and indeed, the cell surface softnesses of the isogenic *S. aureus* pair with different peptidoglycan cross-linking are similar). Accordingly, the status of the current literature is that no reliable

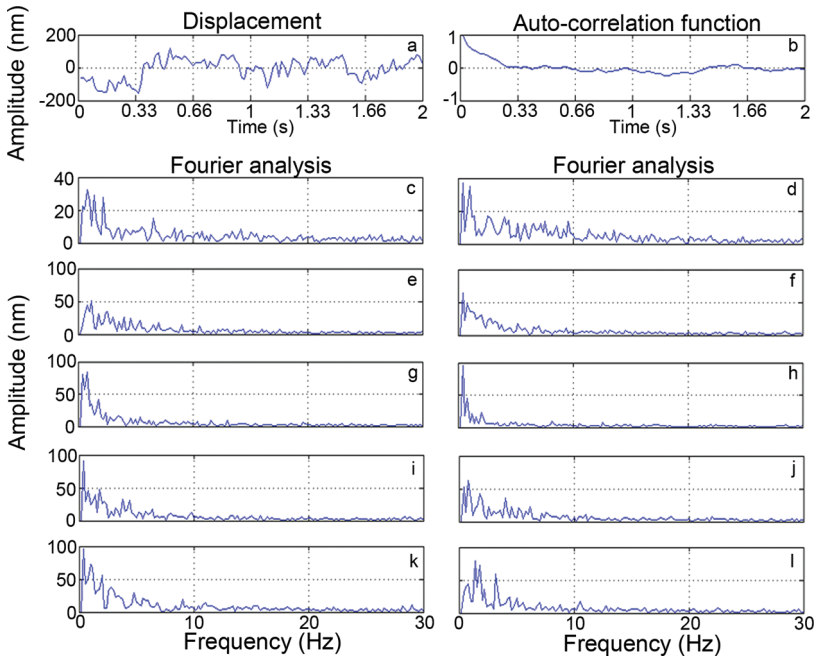

Figure 5. Vibrational displacement, autocorrelation functions, and frequencies of bacterial vibration (example involves *S. salivarius* HB-C12 in a low ionic strength suspension (0.57 mM) under static conditions). (a, b) Examples of time series of vibrational displacement and their autocorrelation functions as a function of time for *S. salivarius* HB-C12 adhering in a low ionic strength suspension (0.57 mM) under static conditions. (c−l) Amplitude of Fourier components as a function of their vibration frequency of nine different, single *S. salivarius* HB-C12 bacteria adhering to glass under the conditions of panels a and b.

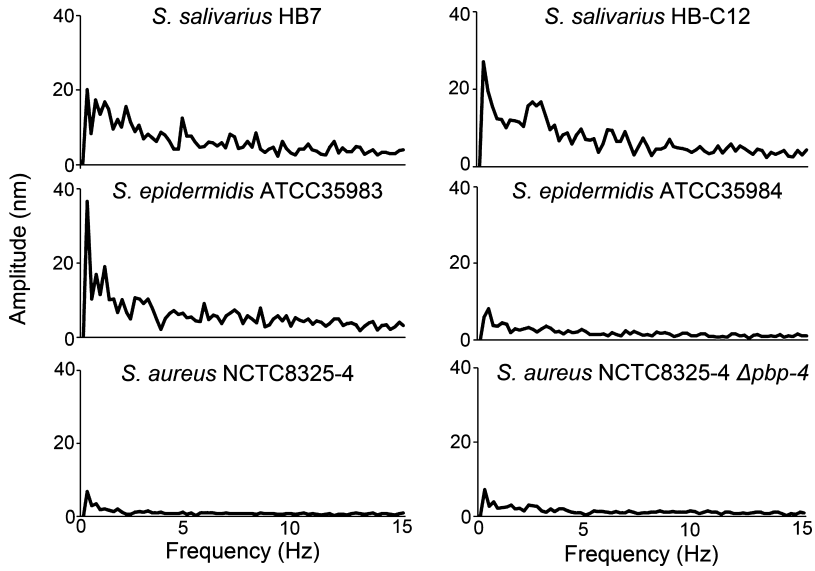

Figure 6. Average amplitudes of Fourier components as a function of their vibration frequencies over five different representatives for each strain. Bacteria were adhering on glass in a low ionic strength suspension (0.57 mM) under static conditions.

method yet exists to derive the viscoelastic properties of the bond between bacteria and substratum surfaces.

The outermost bacterial cell surface is composed of an open network of polyelectrolytes, composed of charged groups along polymer chains of proteins and polysaccharides. Within each pair of strains (compare Figures 4 and 7a), the strain with the smallest electrophoretic softness, that is with the lowest permeability to fluid flow, also possessed the largest spring constants under low ionic strength and static conditions. Note that the electrophoretic softness of *S. aureus* NCTC 8325-4 and its isogenic mutant *S. aureus* NCTC 8325-4 Δ*pbp-4* were identical. The polyelectrolyte nature of the outermost bacterial cell surface suggests that the persistence lengths of the polymer chains in the outermost bacterial cell surface increase with decreasing ionic strength of the suspending fluid as a result of the increased electrostatic repulsion between the chains.[35] This yields expansion of the polyelectrolyte network at low ionic strengths, as illustrated in Figure 8. This

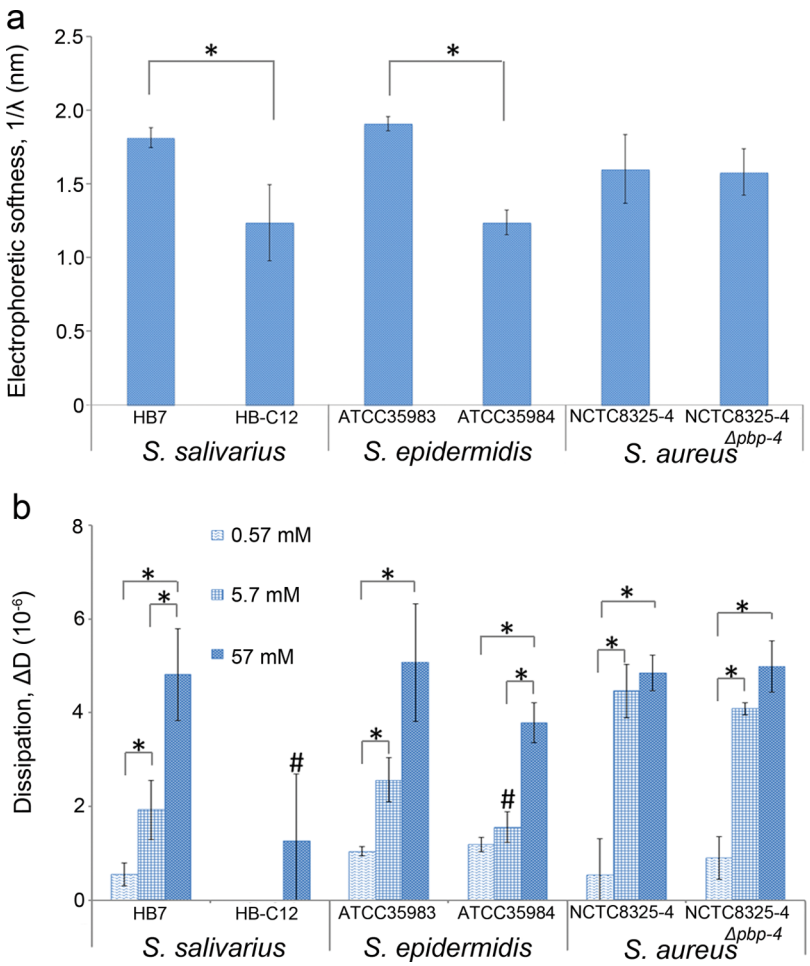

Figure 7. (a) Electrophoretically derived bacterial cell surface softness, $1/\lambda$, of the three pairs of bacterial strains included in this study. (b) Dissipation shift, ΔD, measured by QCM-D at the first overtone and at three ionic strengths. Higher dissipation shifts are associated with larger vibrational damping. No data could be obtained for *S. salivarius* HB-C12 strains at the lowest ionic strengths (0.57 and 5.7 mM) due to low numbers of adhering bacteria. Error bars indicate standard deviations over three experiments with separately cultured bacteria. ∗ indicate significant differences between bacterial surface softness or dissipation shift of the parental and mutant strain or between different ionic strengths, while # indicate significant differences between strains making up a pair.

expansion causes low dissipation shifts in QCM-D (Figure 7b). Low dissipation shifts indicate low vibrational damping, yielding high vibrational amplitudes (Figure 3).

Vibrational amplitudes are largest under static conditions and smaller in the direction of the flow than perpendicular to it, but amplitudes return to their original static values after arresting the flow (not shown). This indicates that under fluid flow the stress−strain relationship is nonlinear,[36] due to reversible deformation of the polyelectrolyte network constituting the outermost cell surface[31] rather than breaking of noncovalent intermolecular bonds, as observed for single proteins.[37] Therefore, the spring constants derived for bacterial bonds under fluid flow, might better be designated as "apparent" spring constants. Under static conditions, vibrations are restricted to the linear regime and spring constants derived represent the spring constant of the bond without influences of a nonlinear component. In the linear regime at low ionic strengths and within each pair of strains, the strain with the smallest electrophoretic softness (Figure 7a) possesses the largest spring constants (Figure 4a).

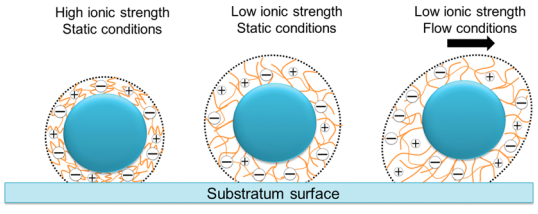

Figure 8. Schematic representation of the outermost bacterial cell layer under static and fluid flow conditions at different ionic strengths. Under high ionic strength conditions, the polyelectrolyte network destabilizes and collapses, damping the vibrational amplitude, while under low ionic strength conditions the network is expanded due to electrostatic repulsion, causing an increase in vibrational amplitude. Under fluid flow conditions, noncovalent intermolecular bonds in the polyelectrolyte are broken and network polymers are stretched causing stiffening of the polymer network surrounding a bacterium and resulting in lower vibrational amplitudes in the direction of flow.

Deriving spring constants of bacterial bonds from bacterial vibrations assumes that the vibrations are

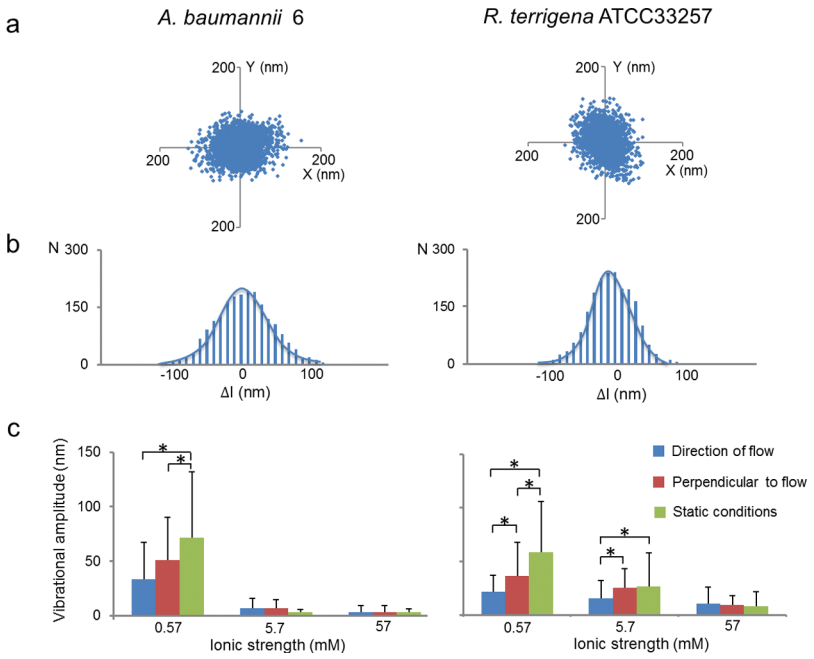

Figure 9. Examples of position maps (a) of a single, adhering Gram-negative bacterium (*A. baumannii* 6 and *R. terrigena* ATCC33257) at various time points under static conditions in a low ionic strength suspension (0.57 mM), together with corresponding distribution histograms of bacterial displacement from their equilibrium positions (b) and resulting vibrational amplitudes (c) at different ionic strengths and under fluid flow. Error bars indicate standard deviations over three experiments with separately cultured bacteria (note that Gram-negative bacteria were cultured in Nutrient Broth under elsewise similar conditions as the Gram-positive strains involved in this study). For each experiment, 30 randomly selected adhering bacteria were analyzed. Distribution histograms were fitted to a Gaussian function. ∗ indicate significant differences between vibrational amplitudes under static conditions and under fluid flow.

related to the strength with which they are attached to the substratum surface rather than to the metabolism of the living bacterium itself. This assumption seems justified because adhering abiotic particles exhibit similar nanoscopic vibrations than do adhering bacteria. Analysis of the nanoscopic vibrational amplitude of abiotic, 2 μm diameter latex particles tethered to a glass surface by polyacrylamide polymeric chains,[17,18] yielded a spring constant in water between 1 to 2×10^{-6} N m^{-1}, which is very similar to that found here for fibrillated streptococci adhering in a low ionic strength buffer under static conditions.

Isogenic Δ*pbp-4* mutants have the same outermost surface properties as their parent strains and accordingly the electrophoretic softness and the dissipation shifts of *S. aureus* NCTC8325-4 and its isogenic mutant *S. aureus* NCTC8325-4 Δ*pbp-4* are identical (see Figure 7). More importantly, the vibrational amplitudes for *S. aureus* NCTC8325-4 and its isogenic mutant *S. aureus* NCTC8325-4 Δ*pbp-4*, deficient in peptidoglycan cross-linking are also nearly identical. This attests to the fact that nanoscopic vibrational amplitudes of adhering bacteria solely reflect the outermost bacterial cell surface layer and not more internal structures. Gram-positive strains, as selected for this study, bear in common that they have a peptidoglycan layer that is relatively thick as compared with the one of Gram-negative strains. In addition, Gram-negative strains possess an inner and outer lipid membrane, whereas Gram-positive strains lack the outer membrane. This raises the question as to whether the outer membrane of Gram-negative bacteria has a specific role in vibrations of adhering bacteria. To answer this question, we carried out experiments with two Gram-negative bacterial strains: *Acinetobacter baumannii* 6 and *Raoutella terrigena* ATCC33257. In Figure 9 it can be seen that both Gram-negative strains demonstrate an entirely similar behavior as do Gram-positive bacteria with respect to the vibrations exhibited in their adhering state. Moreover, also the dependence of their vibrational amplitudes on ionic strength is similar to the one of Gram-positive strains (compare Figures 3 and 9). Accordingly, there is no systematic impact of the outer membrane on vibrations of adhering Gram-negative bacteria and the spring constants with which they adhere to a substratum surface.

The fact that nanoscopic vibrational amplitudes are related to the outermost bacterial cell surface only is a major advantage of vibrational amplitude analysis, as other methods to derive the properties of the adhesive bond between adhering bacteria and a substratum surface not only reflect the bond itself, but also pertain to more internal structures, like the peptidoglycan envelope. Such an influence of more internal structures is indicated for instance by experiments in which deformation is imposed on an adhering bacterium by wrenching it between a substratum surface and the AFM cantilever. Wrenching of bacteria in AFM experiments results in compression forces that almost inevitably

increases the number of binding sites between an adhering bacterium and a surface, yielding higher spring constants than obtained here from analysis of vibrational amplitudes[34] that are measured under the influence of naturally occurring adhesion forces.

In the elastic regime, an adhering bacterium can be considered as a simple mass solely tethered to a substratum surface through an undamped spring. Under these conditions, resonance frequencies, f_0, of adhering bacteria can be calculated using the spring constants k_s derived in this paper according to

$$f_0 = \frac{1}{2\pi}\sqrt{\frac{k_s}{m}} \quad (1)$$

where m is the bacterial mass (around 10^{-15} kg). For the present collection of bacterial strains adhering to a glass substratum, the resonance frequencies calculated on the basis of eq 1 would be in the kHz range (3−37 kHz). Fourier analysis of displacement time series showed vibrational amplitudes at low frequencies (Figures 5 and 6), far too low to be recognized as bacterial resonances. This indicates that vibrations of adhering bacteria are caused by Brownian motion forces, as can also be concluded from the Gaussian distribution of bacterial displacements.

CONCLUSIONS

The present observations show that the polyelectrolyte network constituting the outermost bacterial cell layer determines the nanoscopic vibrational amplitudes of bacteria adhering to substratum surfaces both in Gram-positive as well as in Gram-negative strains. Due to the polyelectrolyte nature of the network, spring constants derived from vibration analyses increase with increasing ionic strengths. In streptococci, the polyelectrolyte network is formed by fibrillar surface appendages and spring constants decrease with increasing fibrillar density on the bacterial cell surface. In staphylococci, EPS is the main network component, and larger amounts of EPS yield higher spring constants. Under flow conditions, as opposite to static ones, bacterial bonds with substratum surfaces are stretched by fluid shear forces exerted on the adhering bacteria in the direction of flow yielding network stiffening, similar to the nanomechanical behavior of lactobacillus under shear.[38] For this reason, the spring constants derived for bacterial bonds under fluid flow might better be designated as "apparent" spring constants that may dictate bacterial detachment phenomena under flow. Brownian motion and accompanying vibrations can either stimulate adhesion or detachment. Therewith, vibrational amplitudes might bear relation with critical nanoscopic features of material surfaces that impact bacterial adhesion and detachment, such as on recently described "easy come, easy go" surfaces.[39] The current study may therefore be helpful in defining dimension of nanoscale topographies to allow or attenuate vibrations of adhering bacteria with an impact on adhesion and detachment.

MATERIALS AND METHODS

Bacterial Culturing and Harvesting. Three pairs of bacterial strains were involved in this study: *S. salivarius* HB7 (possessing proteinaceous fibrils with a length of 91 nm on its outermost surface) and HB-C12 (a mutant of *S. salivarius* HB7 having a bald outermost surface), *S. epidermidis* ATCC35983 (a moderately EPS producing strain) and ATCC35984 (a strong EPS producer), and *S. aureus* NCTC8325−4 and its isogenic mutant *S. aureus* NCTC8325-4 Δ*pbp-4*, deficient in membrane cross-linking. *S. salivarius* was precultured in 10 mL of Todd Hewitt broth (OXOID, Basingstoke, UK), while staphylococci were precultured in 10 mL of Tryptone Soy broth (OXOID). Precultures of *S. salivarius* and *S. epidermidis* were grown for 24 h at 37 °C under static conditions, while *S. aureus* was precultured under shaking (150 rpm). After 24 h, 0.5 mL of a preculture was transferred into 10 mL of fresh medium, and the main culture was inoculated for another 16 h under identical conditions. Bacteria were harvested by centrifugation at 5000*g* for 5 min, washed three times with adhesion buffer (50 mM potassium chloride, 2 mM potassium phosphate and 1 mM calcium chloride) with different ionic strengths (0.57 mM, 5.7 mM and 57 mM) at pH 6.8, and sonicated on ice for 3 × 10 s at 30 W (Vibra cell model 375, Sonics and Material Inc., Danbury, CT). Finally, bacteria were resuspended in adhesion buffer to a concentration of 3×10^8 bacteria per mL, as determined in a Bürker−Türk counting chamber.

Measurement of Vibrational Amplitudes of Adhering Bacteria. Vibrational amplitudes were measured under fluid flow and under static conditions. For measurements under fluid flow, bacteria were allowed to adhere to the glass bottom plate of a parallel plate flow chamber. The flow chamber with channel dimensions 175 × 17 × 0.75 mm was equipped with an image analysis system and has been described in detail previously.[12] The top and bottom plates of the chamber were made of glass. Glass plates were cleaned in 2% RBS (Chemical Products R. Borghgraef S.A., Brussels, Belgium) in an ultrasonic bath and rinsed with methanol and water prior to each experiment. All tubes and the flow chamber were filled with adhesion buffer, while care was taken to remove all air bubbles from the system. Next, the bacterial suspension was circulated through the chamber under pulse-free hydrostatic pressure at a shear rate of 10 s^{-1}. For determination of the vibrational amplitudes of adhering bacteria under static conditions, the bacterial suspension was circulated for 1 h and measurements were taken 15 min after arresting the flow.

Vibration of adhering bacteria was observed with a CCD camera (A101F, Basler AG, Ahrensburg, Germany) mounted on a phase-contrast microscope (BH2-RFCA, Olympus Optical Co., Tokyo, Japan). The camera was coupled to an image analysis program (Matlab, The MathWorks, Natick, MA), recording 60 consecutive images per s. Each image consists of 1392 × 128 pixels on an 8 bit gray scale resulting in 256 gray-values (Figure 1a).

In order to determine bacterial positions, concentric elliptic contour lines were constructed around the images of adhering bacteria, as illustrated in Figure 1b. We used elliptic contour lines, in order to account for possible rotational asymmetries as due to the presence of fluid flow. Subsequently, the centers of these elliptic contour lines were determined, representing the position of a bacterium (see Figure 1c). Bacterial positions were calculated on the basis of 2000 images taken per bacterium over a time-period of 33 s, and the variation in positions observed over time served to analyze their displacement.

In order to account for possible vibrations of the building or microscope, the vibrational amplitude of a fixed marker on the

glass substratum was taken as a reference amplitude, and subtracted from the vibrational amplitudes calculated for adhering bacteria. Negative amplitudes were taken as zero.

The vibrational amplitudes presented represent the average over bacterial vibration amplitudes from three experiments with separate bacterial cultures. Each experiment involved the analysis of the vibration of 30 randomly selected bacteria.

Calculation of Spring Constants from Vibrational Amplitudes. The vibrational displacement of bacteria as a function of time from their equilibrium positions was used to calculate the spring constants of the bond between an adhering bacterium and a substratum surface. To this end, adhering bacteria were assumed to behave as harmonic oscillators, connected to the surface by an elastic, undamped spring with a linear relation between force and displacement

$$F = k_s \Delta l \tag{2}$$

where k_s is the spring constant and Δl the bacterial displacement from its equilibrium position. The energy (E) involved in stretching of the spring is

$$E = \frac{1}{2} k_s \Delta l^2 \tag{3}$$

Because vibrations are considered to result from thermodynamic processes while ignoring viscous damping and assuming the system to be in a thermodynamic equilibrium, the occurrence N of a displacement Δl from a bacterium's equilibrium position is governed by the Boltzman distribution,[16] as described by

$$N = A \exp\left(-\frac{E}{k_B T}\right) = A \exp\left(-\frac{1}{2}\frac{k_s \Delta l^2}{k_B T}\right) \tag{4}$$

where A is a normalization constant, k_B the Boltzmann constant, and T the absolute temperature. Equation 4 represents a Gaussian distribution, and the spring constants can be calculated from the best fit of a Gaussian distribution to the distribution histograms of bacterial displacements (Figure 2b,d) using the Sigmaplot 12.1 (Systat Software, Inc., San Jose, CA).

Autocorrelation and Frequency Analysis of Bacterial Vibrations. Autocorrelation functions of bacterial displacement over time were used to verify the continuity of the vibrational displacement as a function of time over several frames. Fourier transformation of displacement time series was used to determine the frequency spectrum of the bacterial vibrations. Both autocorrelation functions and Fourier transformations were obtained by using Matlab. Each time series analyzed comprised 300 frames (5 s).

Bacterial Cell Surface Softness. In order to calculate the softness of the bacterial cell surfaces, electrophoretic mobilities of the different bacterial strains were measured in KCl solutions of different ionic strengths (0.01, 0.025, 0.05, 0.075, 0.1, and 0.15 M) using particulate microelectrophoresis (Zetasizer nano-ZS; Malvern Instruments, Worcestershire, UK). Prior to each measurement, the pH of the KCl solutions was adjusted to 6.0. Electrophoretic mobilities were measured in triplicate with separate bacterial cultures and the average electrophoretic mobilities as a function of ionic strength were fitted to

$$\mu = \left(\frac{\varepsilon_r \varepsilon_0}{\eta}\right)\left[\left(\frac{\psi_0}{\kappa_m} + \frac{\psi_{DON}}{\lambda}\right)\Big/\left(\frac{1}{\kappa_m} + \frac{1}{\lambda}\right)\right] + \left(\frac{zeN_c}{\eta\lambda^2}\right) \tag{5}$$

in which μ is the electrophoretic mobility, ε_r the relative permittivity, ε_0 the permittivity of vacuum, η the viscosity of the solution, $1/\kappa_m$ the Debye–Hückel length of the polyelectrolyte layer constituting the bacterial cell surface, $1/\lambda$ the softness of the polyelectrolyte layer, inversely related to the friction of liquid flowing in the polyelectrolyte layer, z the valence of charged groups in the polyelectrolyte, e the electrical unit charge, N_c the density of charged groups, ψ_0 the potential at the boundary between the polyelectrolyte layer and the surrounding solution, and ψ_{DON} the Donnan potential within the polyelectrolyte.[23] By taking $1/\lambda$, the softness of the polyelectrolyte layer, and zN_c, the density of charged groups in the polyelectrolyte layer, as parameters of the fit, both $1/\lambda$ and zN_c can be calculated from the electrophoretic mobilities measured as a function of ionic strength using a least-squares curve-fitting routine kindly provided by Prof. Ohshima (Tokyo, Japan). Note that $1/\kappa_m$ is a function of ionic strength and ranges from 3 nm in 0.01 M to 1 nm in 0.1 M KCl for monovalent ions.[40]

QCM-D Measurements. A window-equipped QCM-D flow chamber (Q-sense E1, Q-sense, Gothenburg, Sweden) was used to analyze the energy dissipation of forced oscillations of a silicon dioxide-coated crystal with adhering bacteria. Before an experiment, the silicon dioxide coated crystal was cleaned by washing with 2% (w/v) sodium dodecyl sulfate (SDS) for 15 min. Subsequently, the crystal was washed thoroughly with ultrapure water in a sonicating bath and finally treated with UV/Ozone for 15 min to achieve a water contact angle of zero degrees. Cleaned crystals were immediately housed in the QCM-D flow chamber. After the QCM-D flow chamber was filled with adhesion buffer followed by stabilization of the resonance frequency and dissipation, a bacterial suspension was perfused through the circular QCM-D chamber (diameter 12 mm, height 1 mm) at a flow rate of 17.5 μL s^{-1}, roughly corresponding with a shear rate of 10 s^{-1}, and signal recording was initiated as a function of time. The adhesion process was monitored using a CCD camera (Model A101, Basler vision technologies) mounted on a metallurgical microscope with a 20× objective (Leica DM2500M, Rijswijk, The Netherlands). As soon as the number of adhering bacteria had reached 3×10^6 per cm^2, the dissipation shift was measured at the first overtone of the basic QCM resonance frequency (5 MHz). All measurements were performed in triplicate with separately cultured bacteria of each strain.

Statistical Analysis. All experiments were performed in triplicate with separate bacterial cultures, and all data are presented as means ± standard deviations. Because of the strain selection in this study, results were compared pairwise for the different strains for effects of flow or ionic strength using a Student t test (SPSS Statistics 20, IBM, Armonk, NY). $p < 0.05$ was considered to be statistically significant.

Conflict of Interest: The authors declare the following competing financial interest(s): H.J.B. is also director of a consulting company, SASA BV (GN Schutterlaan 4, 9797 PC Thesinge, The Netherlands).

Acknowledgment. J.S. acknowledges financial support of Project P4.01 NANTICO of the research program of the BioMedical Materials Institute, cofunded by the Ministry of Economic Affairs.

Supporting Information Available: Video of random vibrations of adhering bacteria around the equilibrium position. This material is available free of charge *via* the Internet at http://pubs.acs.org.

REFERENCES AND NOTES

1. Busscher, H. J.; Van der Mei, H. C.; Subbiahdoss, G.; Jutte, P. C.; Van den Dungen, J. J. A. M.; Zaat, S. A. J.; Schultz, M. J.; Grainger, D. W. Biomaterial-Associated Infection: Locating the Finish Line in the Race for the Surface. *Sci. Transl. Med.* **2012**, *4*, 153rv10.
2. Donlan, R. M.; Costerton, J. W. Biofilms: Survival Mechanisms of Clinically Relevant Microorganisms. *Clin. Microbiol. Rev.* **2002**, *15*, 167–193.
3. Flemming, H.; Wingender, J. The Biofilm Matrix. *Nat. Rev. Microbiol.* **2010**, *8*, 623–633.
4. Del Pozo, J.; Patel, R. The Challenge of Treating Biofilm-Associated Bacterial Infections. *Clin. Pharmacol. Ther.* **2007**, *82*, 204–209.
5. Stewart, P. S.; Costerton, W. J. Antibiotic Resistance of Bacteria in Biofilms. *Lancet* **2001**, *358*, 135–138.
6. Busscher, H. J.; Van der Mei, H. C. How Do Bacteria Know They Are on a Surface and Regulate Their Response to an Adhering State? *PLoS Pathog.* **2012**, *8*, e1002440.
7. Rizzello, L.; Sorce, B.; Sabella, S.; Vecchio, G.; Galeone, A.; Brunetti, V.; Cingolani, R.; Pompa, P. P. Impact of Nanoscale Topography on Genomics and Proteomics of Adherent Bacteria. *ACS Nano* **2011**, *5*, 1865–1876.

8. Klayman, B. J.; Volden, P. A.; Stewart, P. S.; Camper, A. K. *Escherichia coli* O157: H7 Requires Colonizing Partner to Adhere and Persist in a Capillary Flow Cell. *Environ. Sci. Technol.* **2009**, *43*, 2105–2111.
9. Xie, X.; Moller, J.; Konradi, R.; Kisielow, M.; Franco-Obregon, A.; Nyfeler, E.; Muhlebach, A.; Chabria, M.; Textor, M.; Lu, Z. H. Automated Time-Resolved Analysis of Bacteria–Substrate Interactions Using Functionalized Microparticles and Flow Cytometry. *Biomaterials* **2011**, *32*, 4347–4357.
10. Coenye, T.; Nelis, H. J. *In Vitro* and *in Vivo* Model Systems To Study Microbial Biofilm Formation. *J. Microbiol. Methods* **2010**, *83*, 89–105.
11. Van Loosdrecht, M. C.; Lyklema, J.; Norde, W.; Zehnder, A. J. Bacterial Adhesion: a Physicochemical Approach. *Microb. Ecol.* **1989**, *17*, 1–15.
12. Busscher, H. J.; Van der Mei, H. C. Microbial Adhesion in Flow Displacement Systems. *Clin. Microbiol. Rev.* **2006**, *19*, 127–141.
13. Walker, S. L.; Hill, J. E.; Redman, J. A.; Elimelech, M. Influence of Growth Phase on Adhesion Kinetics of *Escherichia coli* D21g. *Appl. Environ. Microbiol.* **2005**, *71*, 3093–3099.
14. Hetrick, E. M.; Schoenfisch, M. H. Antibacterial Nitric Oxide-Releasing Xerogels: Cell Viability and Parallel Plate Flow Cell Adhesion Studies. *Biomaterials* **2007**, *28*, 1948–1956.
15. Thomas, W. E.; Trintchina, E.; Forero, M.; Vogel, V.; Sokurenko, E. V. Bacterial Adhesion to Target Cells Enhanced by Shear Force. *Cell* **2002**, *109*, 913–923.
16. Walker, S. L.; Redman, J. A.; Elimelech, M. Role of Cell Surface Lipopolysaccharides in *Escherichia coli* K12 Adhesion and Transport. *Langmuir* **2004**, *20*, 7736–7746.
17. Kamiti, M.; Van de Ven, T. G. M. Measurement of Spring Constants of Polyacrylamide Chains Bridging Particles to a Solid Surface. *Macromolecules* **1996**, *29*, 1191–1194.
18. Dabros, T.; Warszynski, P.; Van de Ven, T. G. M. Motion of Latex Spheres Tethered to a Surface. *J. Colloid Interface Sci.* **1994**, *162*, 254–256.
19. Longo, G.; Alonso-Sarduy, L.; Rio, L. M.; Bizzini, A.; Trampuz, A.; Notz, J.; Dietler, G.; Kasas, S. Rapid Detection of Bacterial Resistance to Antibiotics using AFM Cantilevers as Nanomechanical Sensors. *Nat. Nanotechnol.* **2013**, *8*, 522–526.
20. Lau, P.; Dutcher, J.; Beveridge, T.; Lam, J. Absolute Quantitation of Bacterial Biofilm Adhesion and Viscoelasticity by Microbead Force Spectroscopy. *Biophys. J.* **2009**, *96*, 2935–2948.
21. Klapper, I.; Rupp, C.; Cargo, R.; Purvedorj, B.; Stoodley, P. Viscoelastic Fluid Description of Bacterial Biofilm Material Properties. *Biotechnol. Bioeng.* **2002**, *80*, 289–296.
22. Whitchurch, C. B.; Tolker-Nielsen, T.; Ragas, P. C.; Mattick, J. S. Extracellular DNA Required for Bacterial Biofilm Formation. *Science* **2002**, *295*, 1487–1487.
23. Ohshima, H. Electrophoretic Mobility of Soft Particles. *Colloids Surf. Physicochem. Eng. Aspects* **1995**, *103*, 249–255.
24. Takashima, S.; Morisaki, H. Surface Characteristics of the Microbial Cell of *Pseudomonas syringae* and its Relevance to Cell Attachment. *Colloid. Surf. B* **1997**, *9*, 205–212.
25. Otto, K.; Silhavy, T. J. Surface Sensing and Adhesion of *Escherichia coli* Controlled by the Cpx-signaling Pathway. *Proc. Natl. Acad. Sci. U.S.A.* **2002**, *99*, 2287–2292.
26. Marcus, I. M.; Herzberg, M.; Walker, S. L.; Freger, V. *Pseudomonas aeruginosa* Attachment on QCM-D Sensors: The Role of Cell and Surface Hydrophobicities. *Langmuir* **2012**, *28*, 6396–6402.
27. Schofield, A. L.; Rudd, T. R.; Martin, D. S.; Fernig, D. G.; Edwards, C. Real-Time Monitoring of the Development and Stability of Biofilms of *Streptococcus mutans* using the Quartz Crystal Microbalance with Dissipation Monitoring. *Biosens. Bioelectron.* **2007**, *23*, 407–413.
28. Van der Mei, H. C.; Weerkamp, A. H.; Busscher, H. J. Physicochemical Surface Characteristics and Adhesive Properties of *Streptococcus salivarius* Strains with Defined Cell Surface Structures. *FEMS Microbiol. Lett.* **1987**, *40*, 15–19.
29. Mendez-Vilas, A.; Gallardo-Moreno, A.; González-Martín, M.; Calzado-Montero, R.; Nuevo, M.; Bruque, J.; Perez-Giraldo, C. Surface Characterisation of Two Strains of *Staphylococcus epidermidis* with Different Slime Production by AFM. *Appl. Surf. Sci.* **2004**, *238*, 18–23.
30. Atilano, M. L.; Pereira, P. M.; Yates, J.; Reed, P.; Veiga, H.; Pinho, M. G.; Filipe, S. R. Teichoic Acids are Temporal and Spatial Regulators of Peptidoglycan Crosslinking in *Staphylococcus aureus*. *Proc. Natl. Acad. Sci. U.S.A.* **2010**, *107*, 18991–18996.
31. Motte, S.; Kaufman, L. J. Strain Stiffening in Collagen I Networks. *Biopolymers* **2013**, *99*, 35–46.
32. Vadillo-Rodriguez, V.; Beveridge, T. J.; Dutcher, J. R. Surface Viscoelasticity of Individual Gram-negative Bacterial Cells Measured Using Atomic Force Microscopy. *J. Bacteriol.* **2008**, *190*, 4225–4232.
33. Guhados, G.; Wan, W.; Hutter, J. L. Measurement of the Elastic Modulus of Single Bacterial Cellulose Fibers Using Atomic Force Microscopy. *Langmuir* **2005**, *21*, 6642–6646.
34. Chen, Y.; Norde, W.; Van der Mei, H. C.; Busscher, H. J. Bacterial Cell Surface Deformation Under External Loading. *mBio* **2012**, *3*, e00378–12.
35. Baumann, C. G.; Smith, S. B.; Bloomfield, V. A.; Bustamante, C. Ionic Effects on the Elasticity of Single DNA Molecules. *Proc. Natl. Acad. Sci. U.S.A.* **1997**, *94*, 6185–6190.
36. Chou, T.; Takahashi, K. Non-linear Elastic Behaviour of Flexible Fibre Composites. *Composites* **1987**, *18*, 25–34.
37. Dietz, H.; Berkemeier, F.; Bertz, M.; Rief, M. Anisotropic Deformation Response of Single Protein Molecules. *Proc. Natl. Acad. Sci. U.S.A.* **2006**, *103*, 12724–12728.
38. Tripathi, P.; Beaussart, A.; Alsteens, D.; Dupres, V.; Claes, I.; Von Ossowski, I.; De Vos, W. M.; Palva, A.; Lebeer, S.; Vanderleyden, J. Adhesion and Nanomechanics of Pili from the Probiotic *Lactobacillus rhamnosus* GG. *ACS Nano* **2013**, *7*, 3685–3697.
39. Fang, B.; Jiang, Y.; Rotello, V. M.; Nüsslein, K.; Santore, M. M. Easy Come Easy Go: Surfaces Containing Immobilized Nanoparticles or Isolated Polycation Chains Facilitate Removal of Captured *Staphylococcus aureus* by Retarding Bacterial Bond Maturation. *ACS Nano* **2014**, *8*, 1180–1190.
40. Hiemenz, P. C.; Rajagopalan, R. *Principles of Colloid and Surface Chemistry, Revised and Expanded*; CRC Press: Boca Raton, 1997; Vol. 14.